Supplementary Materials

Cross-linking Network Based on Poly(ethylene oxide): Solid Polymer Electrolyte for Room Temperature Li-Battery

Yuhang Zhang[a], Wei Lu[a], Lina Cong[a], Jia Liu[a], Liqun Sun[a], Alain Mauger[b], Christian M. Julien[b], Haiming Xie[a], and Jun Liu[a**]*

[a] National & Local United Engineering Laboratory for Power Battery, Department of Chemistry, Northeast Normal University Changchun, 130024, China

[b] Sorbonne Université, Institut de Minéralogie, de Physique des Matériaux et de Cosmochimie (IMPMC), CNRS UMR 7590, 4 Place Jussieu, 75005 Paris, France

[*] Corresponding author. E-mail address: xiehm136@nenu.edu.cn (H. Xie)

1. Characterization Methods

The cross-linking content (insoluble fraction) was determined by soaking the membrane sandwiched between two pieces of stainless-steel into acetonitrile (ACN, Sigma-Aldrich) overnight. The non-cross-linked polymer chain components were dissolved, and the final gel content was calculated by dividing the mass of the dry sample left by that of the original. The dissolution process was operated at room temperature with continuous stirring and the removal of solvents was taken at 40 °C in vacuum for several hours. The qualitative investigation of the structure change after the dual-reaction was studied by Fourier transform infrared (FTIR) spectra, which were recorded with a Magna 560 spectrometer (American Nicolet) using the KBr pellet technique. The X-ray diffraction (XRD) patterns were performed on a Rigaku SmartLab Diffractometer with Cu Kα radiation (λ = 1.54056 Å) at a voltage of 40 kV and a current of 30 mA. Differential scanning calorimetry (DSC) curves were recorded in nitrogen atmosphere by using DSC Q20 V24.10 Build 122 manufactured by TA Instrument Inc., USA. Thermogravimetric analysis (TGA) data were acquired using a HENVEN HCT-1/2 instrument under N_2 flow of 100 mL min^{-1} at a ramp rate of 10 °C min^{-1} from 25 to 700 °C. The morphology and microstructure of the samples were obtained on a field emission scanning electron microscopy (FESEM, Hitachi SU8010) equipped with an energy-dispersive X-ray (EDX) detector for elemental analysis and mapping.

Ionic conductivities (σ_i) of solid polymer electrolyte were determined by a.c. impedance spectroscopy analysis of cells equipped with two stainless steel (SS)

blocking electrodes (area = 1.96 cm^2) in the frequency range 1 MHz—1 Hz at open

circuit voltage (OCV) using a P4000 workstation at different temperatures in the

range -20 ≤ T ≤ 70 °C. σ_i was calculated by the relation:

$$\sigma_i = \frac{d}{R_b\, A} \qquad (S1)$$

where d is the electrolyte membrane thickness, R_b is the bulk electrolyte

resistance and A is the surface area of the electrode.

The Li$^+$-ion transference number t_{Li^+} was determined at 25 °C using the method

proposed by Evans et al.[S1] from a combination of chronoamperometry and a.c.

impedance measurements before and after application of a polarization ($\Delta V = 10$ mV)

to a non-blocking symmetric Li/PTT-SPE/Li cell with a membrane thickness of ~100

μm. t_{Li^+} was calculated by the relation:

$$t_{Li^+} = \frac{I_{SS}}{I_0}\left[\frac{\Delta V - I_0 R_E^0}{\Delta V - I_{SS} R_E^{SS}}\right] \qquad (S2)$$

where I_0 is the initial current and I_{ss} is the steady-state current after applying the

ΔV voltage for 3-4 h and R_E^0 and R_E^{SS} are the initial and final interfacial resistance of

electrolyte and electrode, respectively.

2. Exploration of synthesis conditions

We firstly explored the appropriate molecule weight (M_w) of PEO, which can

form homogeneous solution/fluid in quantitative acetonitrile (ACN), thus can be able

to form a uniform membrane. As shown in **Table S1**, the dissolving ability of PEO in

limited amount of solvent decreases with the increase of molecule weight. The

molecule weight below 10^6 g mol^{-1} has acceptable dissolving capacity. While, the

PEO of 10^4 g mol^{-1} is hardly to form a SPE membrane and the distribute of 3×10^5 g mol^{-1} PEO is inferior than 10^5 g mol^{-1}. **Table S2** lists the photographs of SPE films prepared with different reactant weight ratio. To summarize the condition, the optimal M_w of PEO is 10^5 g mol^{-1}. The film gets fragileness and hardness with the increase of rigid TEGDMA, while the film become elastic and stickiness along with the increase of TEGDME. We finally confirm the PEO/TEGDMA/TEGDME = 2/1/2 wt.%.

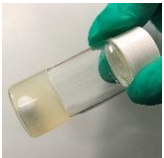**Table S1.** The photographs of mixtures of ACN and PEO with different M_w.
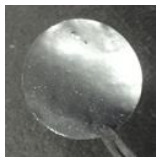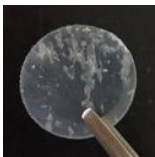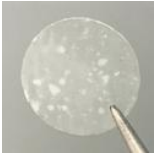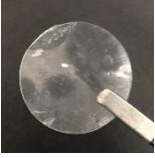
10^4 g mol^{-1}	10^5 g mol^{-1}	3×10^5 g mol^{-1}	10^6 g mol^{-1}	2×10^6 g mol^{-1}

Table S2. The electrolyte film formed by PEO/TEGDMA/TEGDME with different ratio.

M_w (g/mol）	PEO: TEGDMA: TEGDME (weight ratio)			
	1: 1: 0	2: 1: 0	1: 2: 0	1: 1: 1
100,000				
300,000				

3. Interfaces between electrolyte and electrodes

Fig. S1 shows the photographs of electrode/electrolyte (LFP/PTT) composite after hot-press process. The PTT-SPE is *in-situ* formed on the surface of LFP. The

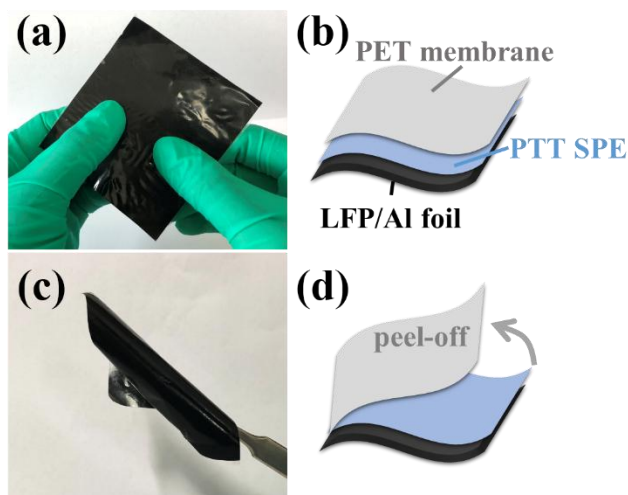LFP/PTT composite is highly flexible and easy to handle.

Fig. S1. Photographs and schematic drawing of electrode/electrolyte (LFP/PTT) composite after hot-pressing: (a, b) with and (c, d) without PET membrane.

As designed, the contact between the solid electrolyte and electrodes is shown in **Fig. S2a**. The PTT-SPE can fit along the particle shape during melting process and then become SPE film by *in-situ* formation, resulting in an optimum interface between PTT-SPE and LFP cathode. For Li metal, the highly flexible SPE film presents excellent adhesion to the side of Li anode. We suppose that the mechanical strength of PTT with close attachment to Li metal can obtain an even current distribution, thus facilitates the homogeneous deposit of Li^+ ions and suppress the growth of lithium dendrite. For the purpose to confirm the advanced interface between SPE and electrodes, cross-sectional FESEM and corresponding energy dispersive spectroscopic (EDS) mapping test were conducted. The entire cell components of LFP cathode (with Al foil), PTT-SPE membrane and Li anode are exhibited in **Fig. S2b**. The SPE layer of about 70 μm is sandwiched between Li anode

and LFP cathode. There are clear boundaries separating the different parts. According to the elemental distribution images in **Fig. S2 (c-e)**, C of polymers are clearly displayed in the middle part, as well as the element F of Li salt, which indicates the uniform dispersion of LiTFSI in the polymer matrix. Fe of LFP cathode are at bottom. The rugged interface implies a sufficient contact between PTT-SPE and LFP cathode, owing to the directly formed SPE on the electrode by hot-pressing and *in-situ* dual-reaction. The tight contact between PTT-SPE and Li anode demonstrates that the soft membrane has a good adhesion to Li metal, thus it can obtain a reduced interfacial resistance and an enhanced cell performance at ambient temperature.
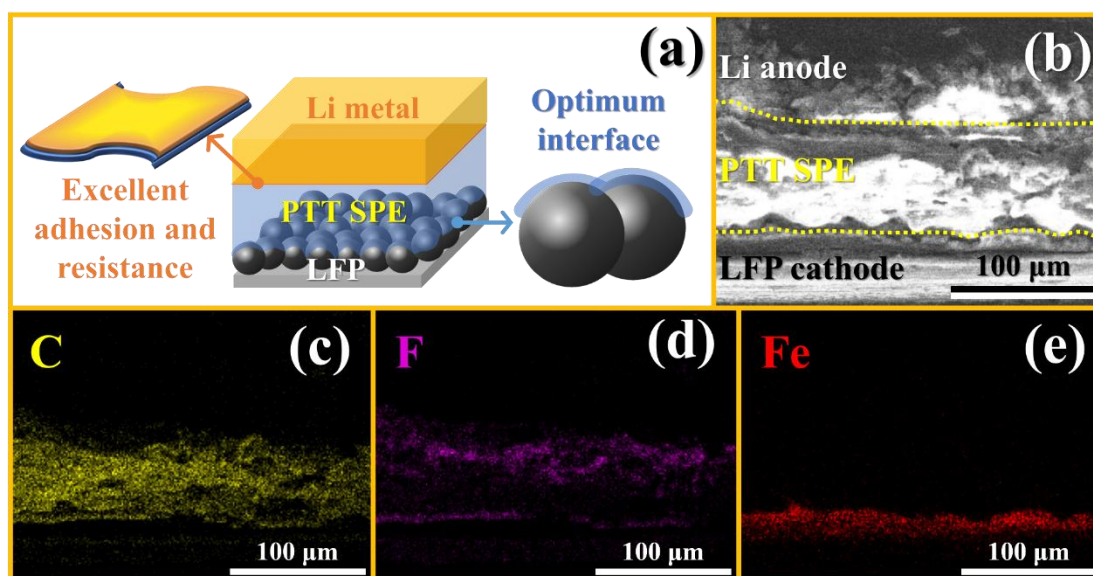

Fig. S2. (a) A schematic representation illustrating the interfaces formed between electrolyte and electrodes. (b-e) Cross-sectional FESEM and corresponding energy dispersive spectroscopic (EDS) mapping images of the configuration inside a cell.

4. Sample Analysis

To confirm the gel content of the UV-derived *in-situ* dual reactions, the PTT-SPE

was sandwiched by two pieces of stain-steel net and soaking in ACN. After string overnight, the non-cross-linked polymer chain components was dissolved, and the final gel content of about 52 wt.% was calculated by dividing the mass of the dry sample left by the weight of the original. The dissolution process was operated at room temperature with continuous stirring and the removal of solvents was taken at 40°C in vacuum for several hours.
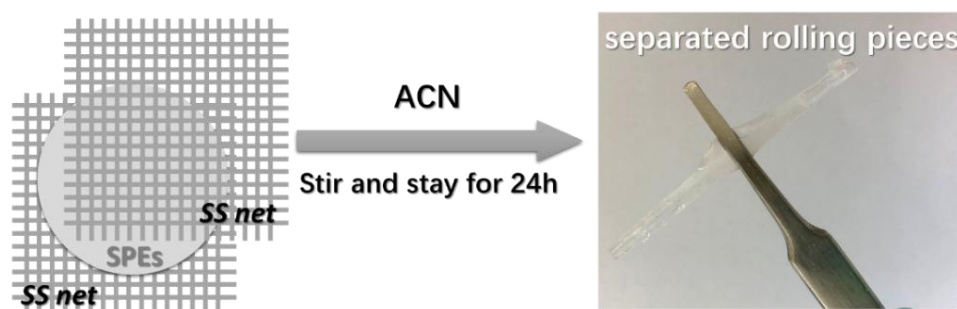

Fig. S3. Illustration of the solution test and the final residuum.

To clarify the FTIR spectra detail of the disappearance of -C=C- after UV, FTIR spectra of photoinitiator (MBP), PTT precursor and PTT-SPE are shown in **Fig. S4**. In order to eliminate the interference of MBP to the PTT precursor, the sample was tested without MBP, denoted as PTT pre (without MBP). The absorption peaks located at 1654, 1602 and 1571 cm^{-1} are assigned to MBP, which exist in the spectrum of PTT sample after UV-derived dual-reaction.
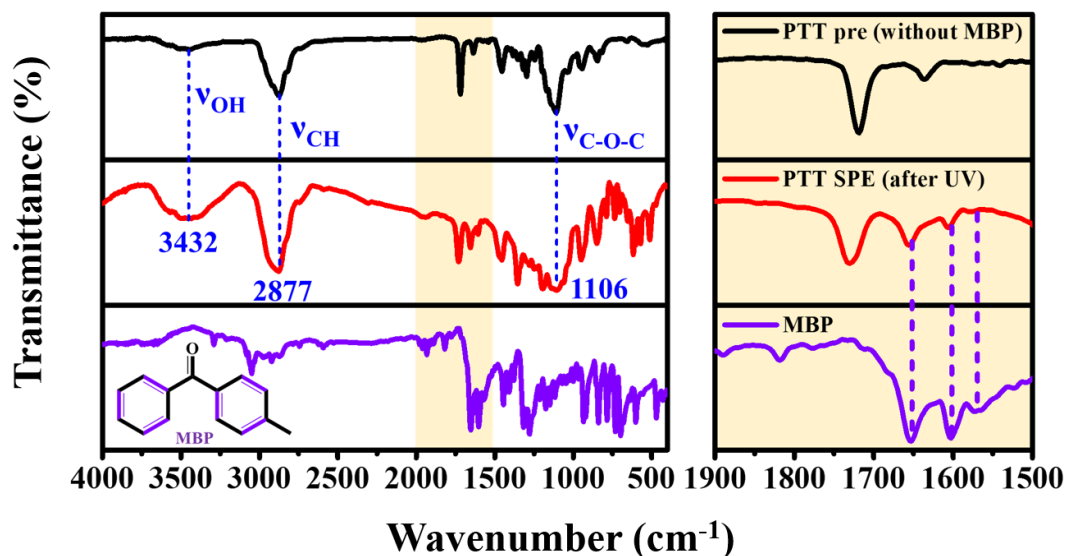
Fig. S4. FTIR spectra of PTT precursor, PTT-SPE and MBP.

The TGA analysis of pristine PEO-SPE, with EO: Li^+ = 20:1 (molar ratio), was measured. As shown in **Fig. S5**, the PEO-SPE keeps stable until 120 °C. The totally weight loss from 120 to 700 °C is 91.5%, which is due to the decomposition of PEO matrix and Li salt. The melting point of PEO-SPE is 59.6 °C according to DTA curve, which means that the ionic conductivity mechanism would be changed at this temperature.
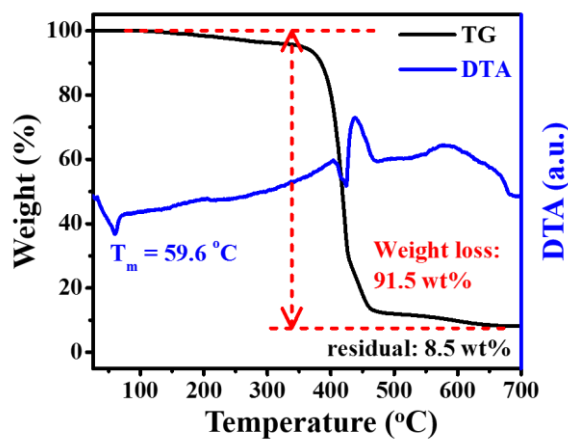

Fig. S5. TG-DTA curves of PEO-SPE (EO: Li^+ = 20:1).

5. EIS Measurements

EIS spectra were collected to identify the reaction elements in a symmetric cell assembled by Li/PTT-SPE/Li. The equivalent circuit models are exhibited in **Fig. S5**. R and C refer to the resistance and corresponding constant phase element (CPE) of different components, respectively. W is the Warburg impedance relate to Li^+-ion diffusion. The fitting results of EIS are listed in **Table S3**.
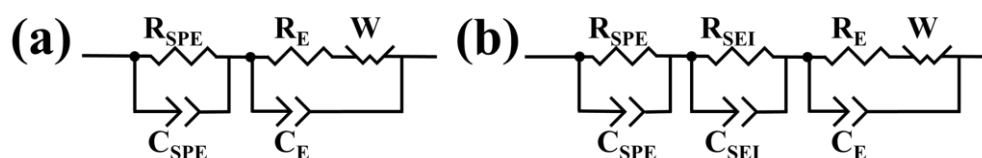

Fig. S6. Equivalent circuit models for Li/PTT-SPE/Li symmetric cell: (a) at fresh stage and (b) after storage.

Table S3. Fitting results of EIS analyses for Li/PTT-SPE/Li symmetric cells.

$R_{\_cal}$	fresh cell	1 d	3 d	5 d	10 d	20 d	30 d	36 d
R_{SPE}/ohm	65	80	82	74	93	93	94	97
C_{SPE}/F	5.2×10^{-8}	1.0×10^{-7}	1.5×10^{-7}	8.5×10^{-8}	4.5×10^{-8}	4.1×10^{-8}	4.1×10^{-8}	4.1×10^{-8}
R_{SEI}/ ohm	-	249	216	208	251	260	259	325
C_{SEI}/F	-	4.0×10^{-6}	3.7×10^{-5}	3.9×10^{-5}	2.8×10^{-5}	3.0×10^{-5}	2.1×10^{-5}	2.3×10^{-5}
R_E/ ohm	487	379	418	420	412	406	390	338
C_E/F	7.0×10^{-6}	5.1×10^{-5}	5.3×10^{-6}	6.4×10^{-6}	6.1×10^{-6}	6.2×10^{-6}	6.4×10^{-6}	6.6×10^{-6}

The equivalent circuit models for LFP/PTT-SPE/Li cells are exhibited in **Fig. S6**

and the fitting results are listed in **Table 4**. The R_{SPE} value calculated from a full cell is 31 Ω, which is much lower than from a symmetric cell. This is attributed to the *in-situ* formation of a thinner SPE film directly onto the LFP cathode.
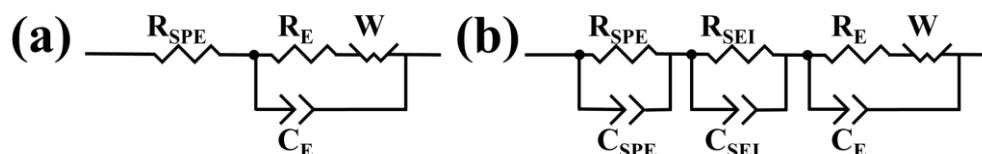

Fig. S7. Equivalent circuit models for LFP/PTT-SPE/Li cell: (a) at fresh stage and (b) after cycles.

Table S4. Fitting results of EIS analyses for LFP/PTT-SPE/Li cells.

$R_{\_cal}$	fresh cell	after 100 cycles
R_{SPE}/ohm	31	151
C_{SPE}/F	-	2.6×10^{-7}
R_{SEI}/ ohm	-	206
C_{SEI}/F	-	3.5×10^{-5}
R_E/ ohm	1476	1295
C_E/F	7.1×10^{-6}	5.1×10^{-6}

6. Electrochemical characteristic of PTT-SPE

The CV curves and galvanostatic charge-discharge profiles (0.1 C) of PTT-SPE and traditional liquid electrolyte (LE) system (PE separator with 1 M LiTFSI in EC/DMC = 1/1 V/V) are shown in **Fig. S7**. The polarization of PTT-SPE is comparable with liquid electrolyte.
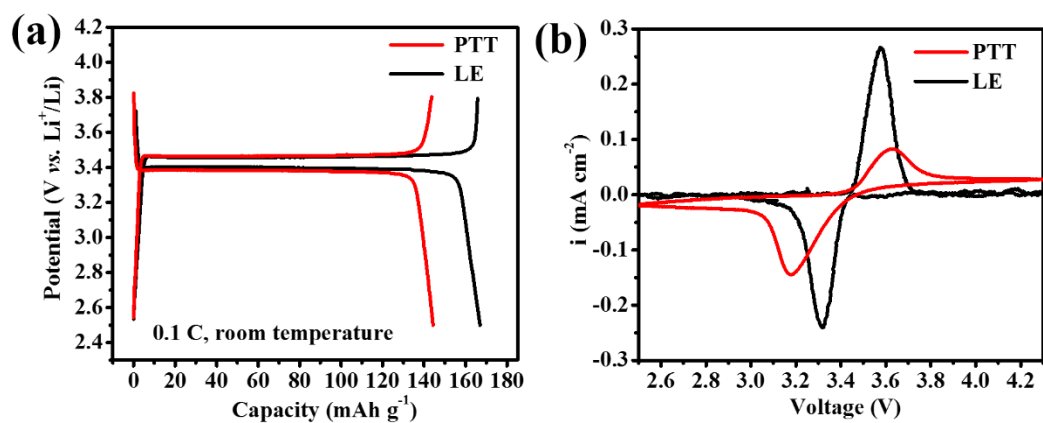
Fig. S8. (a) Charge-discharge profiles and CV curves of LFP/PTT-SPE/Li cell and LFP/LE/Li cell.
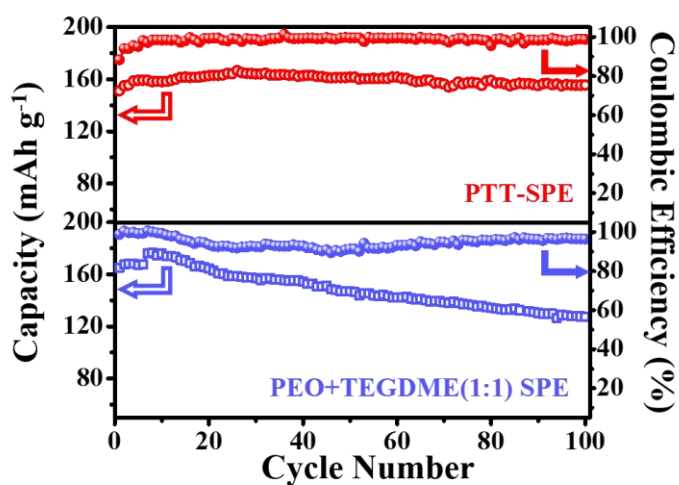

Fig. S9. The long-term cycle performances of PTT-SPE, PEO+TEGDME (1:1) SPE at 0.05 C.

References

[S1] J. Evans, C.A. Vincent, P.G. Bruce, Polymer, 28 (1987) 2324-2328.